Published in final edited form as:
Circulation. 2013 January 29; 127(4): 486–499. doi:10.1161/CIRCULATIONAHA.112.116988.

A Crucial Role for p90RSK-Mediated Reduction of ERK5 Transcriptional Activity in Endothelial Dysfunction and Atherosclerosis

Nhat-Tu Le, Ph.D.[1,*], **Kyung-Sun Heo, Ph.D.**[1,*], **Yuichiro Takei, Ph.D.**[1], **Hakjoo Lee, Ph.D.**[1], **Chang-Hoon Woo, D.V.M., Ph.D.**[1,2], **Eugene Chang, Ph.D.**[1], **Carolyn McClain, BSc**[1], **Cheryl Hurley**[1], **Xin Wang, M.D., Ph.D.**[3], **Faqian Li, B.M., Ph.D.**[4], **Haodong Xu, B.M., Ph.D.**[1,4], **Craig Morrell, Ph.D.**[1], **Mark A. Sullivan, Ph.D.**[5], **Michael S. Cohen, Ph.D.**[6], **Iana M. Serafimova, Ph.D.**[6], **Jack Taunton, Ph.D.**[6], **Keigi Fujiwara, Ph.D.**[1], and **Jun-ichi Abe, M.D., Ph.D.**[1]

[1]Aab Cardiovascular Research Institute, University of Rochester, Rochester, NY

[3]Faculty of Life Sciences, University of Manchester, Manchester M13 9PT, UK

[4]Department of Pathology, University of Rochester, Rochester, NY

[5]Department of Microbiology and Immunology, University of Rochester, Rochester, NY

[6]Howard Hughes Medical Institute and Department of Cellular and Molecular Pharmacology, University of California, San Francisco, San Francisco, CA

Abstract

Background—Diabetes mellitus (DM) is a major risk factor for cardiovascular mortality by increasing endothelial cell (EC) dysfunction and subsequently accelerating atherosclerosis. Extracellular-signal regulated kinase 5 (ERK5) is activated by steady laminar flow and regulates EC function by increasing eNOS expression and inhibiting EC inflammation. However, the role and regulatory mechanisms of ERK5 in EC dysfunction and atherosclerosis are poorly understood. Here, we report the critical role of the p90 ribosomal S6 kinase (p90RSK)/ERK5 complex in EC dysfunction in DM and atherosclerosis.

Methods and Results—Inducible EC-specific ERK5 knockout (ERK5-EKO) mice showed increased leukocyte rolling and impaired vessel reactivity. To examine the role of endothelial ERK5 in atherosclerosis, we used inducible ERK5-EKO-LDLR$^{-/-}$ mice and observed increased plaque formation. When activated, p90RSK associated with ERK5, and this association inhibited ERK5 transcriptional activity and up-regulated VCAM-1 expression. In addition, p90RSK directly phosphorylated ERK5 S496 and reduced eNOS expression. p90RSK activity was increased in diabetic mouse vessels, and FMK-MEA, a specific p90RSK inhibitor, ameliorated EC-leukocyte recruitment and diminished vascular reactivity in DM mice. Interestingly, in ERK-EKO mice,

Correspondence: Jack Taunton, Ph.D. and Jun-ichi Abe, M.D., Ph.D., Jack Taunton, Ph.D.: Program in Chemistry and Chemical Biology, Department of Cellular and Molecular Pharmacology, University of California, San Francisco, California 94158, Phone: 415-514-2004, Fax: (415) 514-0822, taunton@cmp.ucsf.edu, Jun-ichi Abe, M.D., Ph.D.: Aab Cardiovascular Research Institute, 601 Elmwood Ave, Box CVRI, University of Rochester, School of Medicine and Dentistry, Rochester, NY 14642, Phone: (585) 276-9794, Fax: (585) 276-9830, Jun-ichi_abe@urmc.rochester.edu.
[*]These authors contributed equally to this manuscript
[2]Current address: Department of Pharmacology, College of Medicine, Yeungnam University Daegu 705-717, Korea

Conflict of Interest Disclosures: J.T. is a cofounder of Principia Biopharma, which has licensed FMK-MEA.

increased leukocyte rolling and impaired vessel reactivity were resistant to the beneficial effects of FMK-MEA, suggesting a critical role for endothelial ERK5 in mediating the salutary effects of FMK-MEA on endothelial dysfunction. FMK-MEA also inhibited atherosclerosis formation in $ApoE^{-/-}$ mice.

Conclusions—Our study highlights the importance of the p90RSK/ERK5 module as a critical mediator of EC dysfunction in DM and atherosclerosis formation, thus revealing a potential new target for therapeutic intervention.

Keywords

Diabetes mellitus; endothelial dysfunction; p90RSK; ERK5; signal transduction

Introduction

Endothelial dysfunction is commonly observed in patients with diabetes and atherosclerosis[1, 2] and is recognized as an independent risk factor for the development of cardiovascular disease. Enhanced inflammation, generation of reactive oxygen species (ROS), and changes in vasoreactivity are characteristics of endothelial dysfunction[3, 4]. Hyperglycemia is a characteristic feature of DM and plays a critical role in DM-associated microvascular complications[5, 6], including endothelial dysfunction[1, 7]. ERK5 activation induced by steady laminar flow (s-flow) inhibits leukocyte-endothelial interaction and adhesion molecule expression[8–12]. Importantly, ERK5 has not only a kinase domain but also a transcriptional activation domain, the latter of which is regulated by an intra-molecular interaction independent of ERK5 kinase activity[11]. ERK5/MEF2/KLF2 signaling is involved in the s-flow-mediated eNOS expression and anti-inflammatory effects[13].

In this study, we focus on the following two goals to define novel roles for p90RSK and ERK5 in EC pathophysiology: 1) to determine the role of the p90RSK-ERK5 module in endothelial dysfunction and 2) to investigate the role of p90RSK activation (which causes endothelial dysfunction) on atherosclerosis formation.

Methods

Additional details of the experimental Procedures are included in the Supplemental information.

Statistical Analysis

Data are presented as mean ± SEM. Statistical analysis was performed with the GraphPad Prism program, version 4.00 (GraphPad Software, Inc., CA). Nonparametric methods were used to analyze differences between independent groups. Differences between 2 groups were analyzed by Wilcoxon signed-rank test; between > 2 groups were analyzed by Kruskal-Wallis test, followed by Bonferroni multiple-comparison test. (1) the sample size, (2) number of repeated measurements per experiment unit including time intervals, and (3) where the correlation data come from, were listed in each figure and figure legend. P values less than 0.05 are accepted as being statistically significant and indicated by one asterisk (*). Two asterisks indicate the p value less than 0.01 (**). Since large numbers of statistical comparisons were performed, all at the 0.05 level of significance may result in the possibility of a type I error.

Results

High glucose and H_2O_2 synergistically inhibit ERK5-mediated functions in a p90RSK-dependent manner

Previously, we have reported that ROS inhibits ERK5 transcriptional activity[14, 15]. In addition, we also noted that p90RSK is activated by ROS[16]. Therefore, we asked if p90RSK inhibited ERK5 transcriptional activity in ECs. Since substantial evidence has implicated the role for H_2O_2 in promoting EC dysfunction and DM-associated cardiovascular complications[3, 4], we specifically investigated if H_2O_2 inhibits ERK5 transcriptional activity by activating p90RSK[14]. First, in HUVECs, we found that H_2O_2-induced p90RSK activation preceded ERK5 activation (Fig.1A, C, D) and that dominant negative ERK5 had no effect on p90RSK kinase activation (Fig.S1A, B). These data suggest that p90RSK might negatively regulate ERK5 function in ECs in response to H_2O_2, despite the fact that ERK5 has been suggested to be upstream of p90RSK under certain conditions[17].

We found that WT-p90RSK overexpression not only inhibited ERK5 transcriptional activity (measured by co-transfecting ECs with CA-MEK5α, a Gal4-ERK5 fusion construct, and a Gal4-driven luciferase reporter) but also enhanced H_2O_2-mediated inhibition of ERK5 transcriptional activity (Fig.1E). However, the inhibitory effect of H_2O_2 on ERK5 transcriptional activity was dose-dependently abolished by a highly selective inhibitor of p90RSK, fluoromethyl ketone-methoxyethylamine (FMK-MEA)[18] (Fig.1F, S1C, and TableS1), suggesting the crucial role for p90RSK activation in ERK5 transcriptional activity. Because ERK5 enhances MEF2 activity and subsequently KLF2 promoter activity in ECs[19], we also tested the effect of p90RSK activation in this context. Similar to the Gal4-ERK5 reporter, H_2O_2 inhibited ERK5-induced KLF2 promoter activity. Importantly, this inhibitory effect of H_2O_2 was completely reversed by FMK-MEA (Fig.1G), further demonstrating an inhibitory effect of p90RSK kinase activity on ERK5-regulated transcription.

Because H_2O_2 inhibits s-flow-induced ERK5 transcriptional activity, KLF2 promoter activity, and subsequent eNOS expression[14], we next asked whether p90RSK mediates these inhibitory effects. ERK5 is activated by s-flow and regulates EC function by increasing eNOS and KLF2 expression and inhibiting EC inflammation[13]. Induction of the KLF2 and eNOS promoter activities by s-flow was counteracted by H_2O_2, but DN-p90RSK completely reversed this inhibitory effect (Fig.S1D). To model the potential effect of diabetes on p90RSK activation, we also investigated the effect of high glucose (25mM, HG) on endothelial p90RSK activation. We found that exposure to either HG (25mM) or low-dose H_2O_2 (20μM) by itself could not strongly activate p90RSK (Figs.S2A, B and data not shown). However, the combination of low-dose H_2O_2 (20μM) and HG strongly induced p90RSK activation (Figs.S2A and B). Mannitol substitution for D-glucose to control for osmotic changes was without effect. In addition, we found that the HG plus low H_2O_2 condition (HG/low H_2O_2) inhibited ERK5 transcriptional activity in a p90RSK-dependent manner (Fig.S2C). Therefore, we used the HG/low H_2O_2 condition as an in vitro model for studying a combined effect of high glucose and ROS (associated with diabetes) on ECs and analyzed the effect in the context of p90RSK activation. We also used advanced glycogen end-products (AGE) and found the involvement of p90RSK activation in AGE-mediated reduction of ERK5 transcriptional activity (Fig.S2D and E), further suggesting the role of endothelial p90RSK-ERK5 module in DM. In mouse endothelial cells isolated from lungs (MECs), HG/low H_2O_2 inhibited KLF2 mRNA expression, and this effect was reversed by FMK-MEA (Fig.1H). Moreover, FMK-MEA inhibited the HG/low H_2O_2-mediated increase in VCAM-1 mRNA (Fig.1I). Finally, overexpression of dominant negative p90RSK was found to counteract the negative and positive effects of HG/low H_2O_2 on eNOS and VCAM-1 protein levels, respectively (Figs.1J-M). Taken together, these data support a pro-

inflammatory role for p90RSK, which is activated in ECs by stimuli associated with DM (HG and ROS) and which serves to counteract the anti-inflammatory program executed by ERK5.

Pro-inflammatory effects of p90RSK are mediated by complex formation with ERK5

To begin to explore the mechanism by which p90RSK negatively regulates ERK5 transcriptional activity, we first asked if p90RSK associates with ERK5. In HUVECs, endogenous p90RSK co-immunoprecipitated with anti-ERK5 but not with IgG control in a manner that was coincident with active but not inactive p90RSK (Fig.1A, B). Two-hybrid experiments indicated that both the NH_2-terminal kinase (aa1-418) and COOH-terminal transcriptional activation domains (aa571-807) of ERK5 bound to p90RSK, whereas the central segment (aa412-577) did not (Fig.S3A). Consistent with the two-hybrid results, the COOH-terminal fragment (aa571-807) blocked the association between p90RSK and full-length ERK5 in a dose-dependent manner (Fig.2A). Importantly, this inhibitory ERK5 fragment abolished H_2O_2-induced reduction of ERK5 transcriptional activity, whereas the central ERK5 (aa412-577) fragment had no effect (Fig.2B). Taken together, these results indicate that inhibition of ERK5 transcriptional activity depends on p90RSK-ERK5 binding, in addition to p90RSK activation.

Next, to examine the role of p90RSK-ERK5 association in increased VCAM-1 expression, we infected MECs with an adenovirus expressing the ERK5 (aa571-807) fragment and found that it significantly blocked VCAM-1 expression induced by HG/H_2O_2 in MECs (Fig. 2C, D). These data provide consistent evidence that p90RSK-ERK5 association is critical for regulation of VCAM-1 expression by p90RSK activation.

p90RSK inhibits ERK5 transcriptional activity by phosphorylating ERK5-S496

We have reported that p90RSK not only associates with ERK5 but also phosphorylates it at S496[20]. Our analysis using NetPhosK1.0 further identified ERK5-S433, -T475, -S486, and -S489 as potential phosphorylation sites, and in vitro kinase assays using GST-tagged ERK5 mutants suggested that T475 and S486 could also be phosphorylated by p90RSK (data not shown). To determine whether these potential phosphorylation sites are involved in ERK5 transcriptional activity, we tested if p90RSK could inhibit transcriptional activity of ERK5 mutants whose potential phosphorylation sites were substituted by Ala. Only ERK5-S496A was resistant to the inhibitory effect of p90RSK (Fig.2E), demonstrating that p90RSK regulates ERK5 transcriptional activity via S496 phosphorylation.

To investigate whether ERK5-S496 is actually phosphorylated by p90RSK in cells, we generated antibodies specific to ERK5 phosphorylated at S496 as described in methods. Western blotting analyses with this antibody show that overexpression of p90RSK stimulated the phosphorylation of WT but not S496A ERK5 (Fig.2F, G). In addition, in HUVECs phosphorylation of endogenous ERK5-S496 was induced by H_2O_2 and inhibited by FMK-MEA treatment (Fig.2H, I) or Ad-DN-p90RSK transduction (Fig.S3B, C).

To investigate the role of p90RSK-mediated ERK5 phosphorylation in the reduction of s-flow-induced eNOS expression by H_2O_2, we used an adenovirus expressing ERK5-S496A (Ad-ERK5-S496A). Of note, we used a relatively high concentration of H_2O_2 (400μM) in this set of experiments due to the protective effect of ERK5 overexpression on eNOS reduction, as described previously[14]. Ad-ERK5-S496A reversed the reduction of s-flow-induced eNOS expression by H_2O_2 (Fig. 2J, K). These results suggest that p90RSK-mediated ERK5-S496 phosphorylation is crucial for the reduced eNOS expression mediated by H_2O_2.

EC-specific ERK5 depletion induces EC dysfunction and accelerates atherosclerosis

Since systemic knockout of ERK5 is lethal in embryos[21] and adults[15], we generated tamoxifen (4-OHT:4-hydroxytamoxifen)-inducible EC-specific ERK5 knockout mice (ERK5-EKO) as described in the Methods section. Sustained reduction of endothelial ERK5 was confirmed by Western blotting using MECs two weeks after 4-OHT injection (Fig.3A). In the spleen lysate of inducible ERK5-EKO$^{-/-}$ mice, we found no reduction of ERK5 compared to that of the VE-Cad-CreER^{T2}-WT control after two weeks of 4-OHT injection, also indicating the reduced ERK5 is endothelial specific (Fig.3B).

ERK5 has been shown to be a critical regulator of KLF2, which in turn regulates eNOS expression and counteracts EC inflammation[13, 14] *in vitro*. We, therefore, assayed the expression of anti- and pro-inflammatory factors in inducible ERK5-EKO$^{+/-}$ mice after two weeks of 4-OHT injection. eNOS expression was decreased while the expression of VCAM-1 and E-selectin was increased in MECs isolated from 4-OHT-treated mice compared to that of vehicle-treated mice (Fig.3A). With regard to apoptosis, no difference was noted in the basal level of cleaved caspase-3 expression or TUNEL-positive cells in the two groups of mice (Fig.3A, S4A). To exclude possible deleterious effects of 4-OHT on ECs, we used non-inducible EC-specific ERK5 knockout mice (VE-Cad-Cre/ERK5$^{flox/flox}$; non-inducible ERK5-EKO$^{-/-}$) that were of the same age as the 4-OHT inducible animals. We found similar effects on eNOS, VCAM-1, and E-selectin expression as in the inducible ERK5-EKO$^{+/-}$ mice (Fig.S4B). Up to 6 months of age, we did not observe any differences in size or body weight between homo- or heterozygous ERK5-EKO mice and non-transgenic littermate control mice, and no notable differences were found on their development, life span, and tissue structures at a gross anatomical level. In addition, we found no differences in the expression of ERK5, eNOS, VCAM-1, E-selectin, total and phospho-p90RSK (Ser380) between vehicle- and 4-OHT-treated VE-Cad-CreER^{T2}/WT mice (Fig.S4C).

To evaluate a functional role of the reduced endothelial ERK5, we studied leukocyte rolling and acetylcholine (Ach)-induced vasodilation in the mesentery of inducible ERK5-EKO$^{+/-}$ mice. Leukocyte rolling was increased in the 4-OHT-treated group compared to that of the vehicle-treated group (Fig.3D, and supplemental video 1). No changes were observed in venular diameter or shear rate under these conditions (Fig.3C). Ach-induced vasodilation was significantly decreased in both inducible heterozygous ERK5-EKO$^{+/-}$ and homozygous ERK5-EKO$^{-/-}$ mice compared to the 4-OHT-treated control VE-Cad-CreER^{T2}/wild type mice (Fig.3E). It is remarkable that phenotypes with inducible KO of one allele and constitutive KO of both alleles are identical, suggesting that ECs are extremely sensitive to ERK5 dosage. EC-independent vasodilation by sodium nitroprusside (SNP) was indistinguishable between inducible ERK5-EKO and VE-Cad-CreER^{T2}/WT mice (Fig.S4D), indicating the critical role of ERK5 in EC-mediated vasodilation.

To examine the role of endothelial ERK5 in atherosclerosis formation, inducible ERK5-EKO-LDLR$^{-/-}$ mice were fed with high cholesterol diet (HCD) for 16 weeks. Compared to the control mice, no difference either in body weight (Fig.S5A), glucose tolerance test (Fig.S5B), or plasma cholesterol level (Fig.S5C) in inducible ERK5-EKO$^{-/-}$; LDLR$^{-/-}$ mice was noted. However, we observed a significant increase in both surface area and size of lesions in the aortic root of these mice compared to that of the control (Fig.3F). These data suggest a critical role of ERK5 in EC dysfunction and subsequent atherosclerosis formation.

p90RSK expression and phosphorylation are increased in DM mouse aorta

To confirm that diabetes increases endothelial p90RSK activation, we analyzed the localization and expression of both total and phospho-p90RSK (p-p90RSK) in *en face*

preparations of mouse endothelium derived from streptozotocin (STZ)-induced diabetic mice (Fig.4A) using a laser scanning confocal microscope. The STZ effect in inducing diabetes in mice was confirmed by the increase in blood glucose levels. This increase was reduced to the normal level when STZ-injected mice were treated twice daily with insulin (Humalin N, 5 IU/kg) after 3 days of STZ injection (Fig.4B).

Fig.4A shows the effect of hyperglycemia on both p-p90RSK and total p90RSK expressions in vehicle-, STZ−, and STZ + insulin-treated mice in the same steady laminar flow area (greater curvature area at aortic arch). The anti-p-p90RSK staining signal was significantly increased in STZ treated mice. Note that both p-p90RSK (upper panels) and total p90RSK (Lower panels) are mainly localized in the nucleus. Based on fluorescence staining intensities, there was a significant decrease in p-p90RSK in aortae derived from insulin-treated diabetic mice compared to that of the untreated mice (Fig.4A, C-D). Furthermore, we detected the endothelial p90RSK activation in MECs isolated from STZ-treated mice by Western blotting and confirmed a significant increase in p90RSK activation compared with vehicle treated mice (Fig.4E). Taken together, these data suggest that the observed increase in p90RSK activation in STZ-treated mice is due to hyperglycemia.

FMK-MEA, a selective p90RSK inhibitor, reverses DM-mediated EC dysfunction

Leukocyte rolling and adhesion are characteristics of vascular inflammation, and vascular reactivity to ACh is an indicator of vascular function. Increased leukocyte rolling[22] and decreased ACh-induced vasodilation[23] in DM have been reported. In STZ-treated mice, leukocyte rolling was increased and ACh-induced vasodilation was dampened compared to those of the vehicle-treated mice (Fig.5A-C, and supplemental video 2). To study the involvement of p90RSK activation in the observed vascular inflammation and dysfunction in STZ-treated mice, FMK-MEA was used. FMK-MEA (Fig.S6A) is a more soluble and metabolically stable version of FMK[19], a selective and irreversible inhibitor of p90RSK1, p90RSK2, and p90RSK4. To show the specificity of FMK-MEA, we used the Ambit/DiscoverX platform to screen 443 kinases and measured the apparent binding constant (Kd) to a given inhibitor. We found that all kinases except RSK1/4 CTD bound with Kd $\gg$ 1μM, which was carried out in vitro against recombinant kinase domains (TableS1). Treatment of mice with FMK-MEA at the highest dose of 50mg/kg inhibited p90RSK1 by >95% and p90RSK2 by ~80% in mouse heart tissue (Fig.S6B). First, we found that the increase of p90RSK activation in MECs isolated from STZ-treated mice was significantly inhibited by FMK-MEA treatment (Fig.4E). Next, we observed a dose-dependent inhibitory effect of FMK-MEA on leukocyte rolling in diabetic mice (Fig.5A-C, and supplemental video 2). The dose dependence of this effect correlated with p90RSK1/2 inhibition (Fig.S6B). Insulin treatment also reduced leukocyte rolling (Fig.5A-C, and supplemental video 2), in agreement with *in vitro* data suggesting that increased leukocyte rolling and adhesion is caused by high glucose[24] and not by STZ side effects. FMK-MEA affected neither systemic leukocyte counts nor blood glucose levels (Fig.S6C, D), demonstrating that FMK-MEA's effect on leukocyte rolling/adhesion is independent of glucose lowering, unlike insulin, and does not result from global inhibition of leukocyte trafficking. By examining ACh-induced vasodilation, a surrogate for EC function, we found that FMK-MEA treatment significantly reversed EC dysfunction induced by hyperglycemia (Fig.5D). Of note, vasodilation induced by sodium nitroprusside was the same in STZ-treated and control mice (Fig.S6E).

To determine the role of p90RSK activation in the expression of pro-inflammatory adhesion molecules and anti-inflammatory eNOS in DM mice, we quantified mRNA levels of VCAM-1, E-selectin, and eNOS in MECs isolated from STZ-induced DM or control mice. STZ diabetic mice exhibited a higher VCAM-1 and E-selectin mRNA expression but a lower eNOS mRNA expression, compared to that of the control mice (Fig.5E-G). Strikingly, FMK-MEA reversed the effect of STZ-induced DM on the expression of VCAM-1, E-

selectin, and eNOS (Fig.5E-G). We confirmed that FMK-MEA treatment resulted in reduced E-selectin expression at the protein level as well (Fig.5H).

To confirm the importance of p90RSK activation in EC function in another DM model, we utilized C57BL/6J-Ins2^{Akita}(Akita) mice, known to be hyperglycemic at 7 weeks of age[25] (Fig.6A). Similar to STZ-treated mice, enhanced recruitment of leukocytes to EC and EC dysfunction were observed in Akita mice compared to age-matched littermate control (Fig. 6B, and supplemental video 3). FMK-MEA treatment significantly decreased leukocyte rolling and improved ACh-induced vasodilation (Fig.6B, C, and supplemental video 3). Using molecular approaches, we generated endothelial specific VE-Cad-CreER^{T2}-WT-p90RSK-Tg mice (EC-WT-p90RSK-Tg) to further ascertain these observations. In the inducible EC-WT-p90RSK-Tg mice, we confirmed increasedp90RSK expression after 4-OHT treatment compared with VE-Cad-CreER^{T2}-WT control mice (Fig.6D). We found that leukocyte rolling in the inducible EC-WT-p90RSK-Tg mice was significantly upregulated than VE-Cad-CreER^{T2}-WT control mice after 4-OHT injection (Fig.6E, and supplemental video 4). Taken together, our findings indicate a critical role for p90RSK activation in EC inflammation and dysfunction in the diabetic state.

EC-specific ERK5 depletion eliminates the beneficial effect of FMK-MEA

To test whether ERK5 mediates the beneficial effects of FMK-MEA in DM-induced inflammatory events, we assayed leukocyte rolling and Ach-induced vasodilation in inducible ERK5-EKO$^{-/-}$ mice with STZ-induced diabetes. Leukocyte rolling was increased and Ach-induced vasodilation was decreased in 4-OHT treated mice (Fig.7A-C, and supplemental video 5). Interestingly, FMK-MEA had no effect on leukocyte rolling and vessel reactivity in this context (Fig.7A-C, and supplemental video 5), suggesting a critical role for endothelial ERK5 in mediating the salutary effects of FMK-MEA on DM-induced endothelial dysfunction.

FMK-MEA inhibits atherosclerosis formation

As p90RSK activation is critical for DM-mediated EC inflammation and dysfunction, processes well known to initiate atherogenesis[1, 26], we explored the role for p90RSK activation in atherogenesis. Atherosclerosis was induced in ApoE$^{-/-}$ mice as described in the Methods[27]. With a normal chow diet and low-dose angiotensin II (Ang II), atherosclerosis was accelerated without abdominal aorta aneurysms (AAA). Under those conditions, FMK-MEA significantly inhibited the formation of atherosclerotic lesions (Fig. 8A). No difference in plasma cholesterol levels was observed in experimental groups (Fig.S6F). With a high fat diet and high-dose Ang II, both atherosclerosis and AAA were noted (Fig.8B). Again, FMK-MEA inhibited atherosclerosis formation in the arch and upper part of the descending aorta (Fig.8B). However, no inhibitory effect of FMK-MEA was observed on AAA formation (data not shown).

DISCUSSION

We have identified two key molecules that are involved in DM-mediated EC dysfunction and a drug that disrupts the regulatory connections between these molecules. Our study strongly suggests that DM activates p90RSK, which directly inhibits the transcriptional activity of ERK5, an atheroprotective non-classical MAP kinase. This induces inflammatory responses in ECs and promotes vascular dysfunction. First, we found a significant increase in leukocyte rolling and reduction in vessel reactivity in mesenteric vessels of inducible ERK5-EKO mice. Next, increased p90RSK activity in ECs was induced by HG both *in vivo* and *in vitro*. FMK-MEA, a specific inhibitor of p90RSK, counteracted DM-mediated EC inflammation and dysfunction, indicating the key role of p90RSK activation in DM.

Interestingly, FMK-MEA could not improve these conditions in ERK5-EKO mice, suggesting the critical role of ERK5 in FMK-MEA-mediated improvement of EC function. Last, we found that FMK-MEA significantly inhibited, and the depletion of endothelial ERK5 accelerated, atherosclerosis formation in ApoE$^{-/-}$ and LDL$^{-/-}$ mice, confirming the importance of the p90RSK-ERK5 module in clinically-relevant endpoints of atherosclerosis.

We think that these data provide strong evidence for the key role of the p90RSK-ERK5 module in endothelial dysfunction and atherosclerosis formation. Although the role of this module on endothelial dysfunction in vivo was further demonstrated by eliminating the beneficial effect of FMK-MEA in EC-specific ERK5 depletion mice, the role of endothelial ERK5 in p90RSK-mediated atherosclerosis formation remains unclear. Further investigation will be necessary to prove this.

An expanded Discussion section is available in the Online Data Supplement.

Supplementary Material

Refer to Web version on PubMed Central for supplementary material.

Acknowledgments

The authors thank Drs. Scott Cameron and Jane Sottile and Ms. Mary Jackson for critically reading our manuscript, and Dr. Cathy Tournier for providing ERK5$^{flox/flox}$ mice.

Funding Sources: This work is supported by grants from the America Heart Association to Dr. Le (Postdoctoral fellowship 10POST4360007), and Dr. Woo (Postdoctoral fellowship 0625957T, Scientist Development Grant 0930360N), and from the National Institutes of Health to Dr. Abe (HL-088637, HL-064839, and HL-077789), and Dr. Taunton (GM-071434). Dr. Abe is a recipient of Established Investigator Awards of the American Heart Association (0740013N).

References

1. Geraldes P, King GL. Activation of protein kinase c isoforms and its impact on diabetic complications. Circ Res. 2010; 106:1319–1331. [PubMed: 20431074]
2. Kim JA, Montagnani M, Koh KK, Quon MJ. Reciprocal relationships between insulin resistance and endothelial dysfunction: Molecular and pathophysiological mechanisms. Circulation. 2006; 113:1888–1904. [PubMed: 16618833]
3. Cai H, Harrison DG. Endothelial dysfunction in cardiovascular diseases: The role of oxidant stress. Circ Res. 2000; 87:840–844. [PubMed: 11073878]
4. Yao D, Brownlee M. Hyperglycemia-induced reactive oxygen species increase expression of the receptor for advanced glycation end products (rage) and rage ligands. Diabetes. 2010; 59:249–255. [PubMed: 19833897]
5. Lusis AJ. Atherosclerosis. Nature. 2000; 407:233–241. [PubMed: 11001066]
6. Hink U, Li H, Mollnau H, Oelze M, Matheis E, Hartmann M, Skatchkov M, Thaiss F, Stahl RA, Warnholtz A, Meinertz T, Griendling K, Harrison DG, Forstermann U, Munzel T. Mechanisms underlying endothelial dysfunction in diabetes mellitus. Circ Res. 2001; 88:E14–E22. [PubMed: 11157681]
7. Srinivasan S, Hatley ME, Bolick DT, Palmer LA, Edelstein D, Brownlee M, Hedrick CC. Hyperglycaemia-induced superoxide production decreases enos expression via ap-1 activation in aortic endothelial cells. Diabetologia. 2004; 47:1727–1734. [PubMed: 15490108]
8. Hayashi M, Kim SW, Imanaka-Yoshida K, Yoshida T, Abel ED, Eliceiri B, Yang Y, Ulevitch RJ, Lee JD. Targeted deletion of bmk1/erk5 in adult mice perturbs vascular integrity and leads to endothelial failure. J Clin Invest. 2004; 113:1138–1148. [PubMed: 15085193]

9. Gimbrone MA Jr, Topper JN, Nagel T, Anderson KR, Garcia-Cardena G. Endothelial dysfunction, hemodynamic forces, and atherogenesis. Ann N Y Acad Sci. 2000; 902:230–239. discussion 239–240. [PubMed: 10865843]
10. Davies PF. Hemodynamic shear stress and the endothelium in cardiovascular pathophysiology. Nat Clin Pract Cardiovasc Med. 2009; 6:16–26. [PubMed: 19029993]
11. Akaike M, Che W, Marmarosh NL, Ohta S, Osawa M, Ding B, Berk BC, Yan C, Abe J. The hinge-helix 1 region of peroxisome proliferator-activated receptor gamma1 (ppargamma1) mediates interaction with extracellular signal-regulated kinase 5 and ppargamma1 transcriptional activation: Involvement in flow-induced ppargamma activation in endothelial cells. Mol Cell Biol. 2004; 24:8691–8704. [PubMed: 15367687]
12. Yamawaki H, Lehoux S, Berk BC. Chronic physiological shear stress inhibits tumor necrosis factor-induced proinflammatory responses in rabbit aorta perfused ex vivo. Circulation. 2003; 108:1619–1625. [PubMed: 12963644]
13. Parmar KM, Larman HB, Dai G, Zhang Y, Wang ET, Moorthy SN, Kratz JR, Lin Z, Jain MK, Gimbrone MA Jr, Garcia-Cardena G. Integration of flow-dependent endothelial phenotypes by kruppel-like factor 2. J Clin Invest. 2006; 116:49–58. [PubMed: 16341264]
14. Woo CH, Shishido T, McClain C, Lim JH, Li JD, Yang J, Yan C, Abe J. Extracellular signal-regulated kinase 5 sumoylation antagonizes shear stress-induced antiinflammatory response and endothelial nitric oxide synthase expression in endothelial cells. Circ Res. 2008; 102:538–545. [PubMed: 18218985]
15. Itoh S, Ding B, Bains CP, Wang N, Takeishi Y, Jalili T, King GL, Walsh RA, Yan C, Abe J. Role of p90 ribosomal s6 kinase (p90rsk) in reactive oxygen species and protein kinase c {beta} (pkc-{beta})-mediated cardiac troponin i phosphorylation. J Biol Chem. 2005; 280:24135–24142. [PubMed: 15840586]
16. Abe J, Okuda M, Huang Q, Yoshizumi M, Berk BC. Reactive oxygen species activate p90 ribosomal s6 kinase via fyn and ras. J Biol Chem. 2000; 275:1739–1748. [PubMed: 10636870]
17. Ranganathan A, Pearson GW, Chrestensen CA, Sturgill TW, Cobb MH. The map kinase erk5 binds to and phosphorylates p90 rsk. Arch Biochem Biophys. 2006; 449:8–16. [PubMed: 16626623]
18. Cuello F, Snabaitis AK, Cohen MS, Taunton J, Avkiran M. Evidence for direct regulation of myocardial na+/h+ exchanger isoform 1 phosphorylation and activity by 90-kda ribosomal s6 kinase (rsk): Effects of the novel and specific rsk inhibitor fmk on responses to alpha1-adrenergic stimulation. Mol Pharmacol. 2007; 71:799–806. [PubMed: 17142297]
19. Kasler HG, Victoria J, Duramad O, Winoto A. Erk5 is a novel type of mitogen-activated protein kinase containing a transcriptional activation domain. Mol Cell Biol. 2000; 20:8382–8389. [PubMed: 11046135]
20. Le NT, Takei Y, Shishido T, Woo CH, Chang E, Heo KS, Lee H, Lu Y, Morrell C, Oikawa M, McClain C, Wang X, Tournier C, Molina CA, Taunton J, Yan C, Fujiwara K, Patterson C, Yang J, Abe J. P90rsk targets the erk5-chip ubiquitin e3 ligase activity in diabetic hearts and promotes cardiac apoptosis and dysfunction. Circulation research. 2012; 110:536–550. [PubMed: 22267842]
21. Sohn SJ, Sarvis BK, Cado D, Winoto A. Erk5 mapk regulates embryonic angiogenesis and acts as a hypoxia- sensitive repressor of vascular endothelial growth factor expression. J Biol Chem. 2002; 277:43344–43351. [PubMed: 12221099]
22. Booth G, Stalker TJ, Lefer AM, Scalia R. Mechanisms of amelioration of glucose-induced endothelial dysfunction following inhibition of protein kinase c in vivo. Diabetes. 2002; 51:1556–1564. [PubMed: 11978656]
23. Taylor PD, Wickenden AD, Mirrlees DJ, Poston L. Endothelial function in the isolated perfused mesentery and aortae of rats with streptozotocin-induced diabetes: Effect of treatment with the aldose reductase inhibitor, ponalrestat. Br J Pharmacol. 1994; 111:42–48. [PubMed: 8012723]
24. Morigi M, Angioletti S, Imberti B, Donadelli R, Micheletti G, Figliuzzi M, Remuzzi A, Zoja C, Remuzzi G. Leukocyte-endothelial interaction is augmented by high glucose concentrations and hyperglycemia in a nf-kb-dependent fashion. J Clin Invest. 1998; 101:1905–1915. [PubMed: 9576755]

25. Yoshioka M, Kayo T, Ikeda T, Koizumi A. A novel locus, mody4, distal to d7mit189 on chromosome 7 determines early-onset niddm in nonobese c57bl/6 (akita) mutant mice. Diabetes. 1997; 46:887–894. [PubMed: 9133560]

26. Yan SF, Ramasamy R, Naka Y, Schmidt AM. Glycation, inflammation, and rage: A scaffold for the macrovascular complications of diabetes and beyond. Circ Res. 2003; 93:1159–1169. [PubMed: 14670831]

27. Daugherty A, Manning MW, Cassis LA. Angiotensin ii promotes atherosclerotic lesions and aneurysms in apolipoprotein e-deficient mice. J Clin Invest. 2000; 105:1605–1612. [PubMed: 10841519]

Epidemiological studies over the past decade have shown that diabetes (DM) significantly affects the process of atherosclerosis formation and following cardiovascular events. Endothelial cell (EC) dysfunction and inflammation are blamed for the pathogenesis of atherosclerosis and cardiovascular complications in diabetic patients, and anti-inflammatory therapy has gained increasing attention in the drug development for cardiovascular diseases. Voluminous evidence showing that diabetic condition activates proinflammatory signaling pathways, but little is known about diabetes-mediated inhibition of anti-inflammatory responses that are activated by factors such as steady laminar flow (s-flow). Our study strongly suggests that DM activates p90RSK, which directly inhibits s-flow-induced transcriptional activation of ERK5, an atheroprotective non-classical MAP kinase. This inhibition induces inflammatory responses in ECs and promotes EC dysfunction. FMK-MEA, a specific inhibitor of p90RSK, counteracted DM-mediated EC inflammation and dysfunction, suggesting p90RSK activation as a key harmful event in DM. Interestingly, FMK-MEA could not improve these conditions in endothelial specific ERK5 knockout mice, indicating a critical role of ERK5 in FMK-MEA-mediated improvement of EC function. FMK-MEA significantly inhibited, and the depletion of endothelial ERK5 accelerated, atherosclerosis formation in $ApoE^{-/-}$ and $LDL^{-/-}$ mice, confirming the importance of the p90RSK-ERK5 module in clinically-relevant endpoints of atherosclerosis. The p90RSK-ERK5 module should be an attractive drug target since it has unique features that distinguish it from other classical MAPK signaling. We believe that regulating ERK5 transcriptional activity is critical for controlling EC inflammation and dysfunction, which should provide a new therapeutic strategy for reducing atherosclerosis.

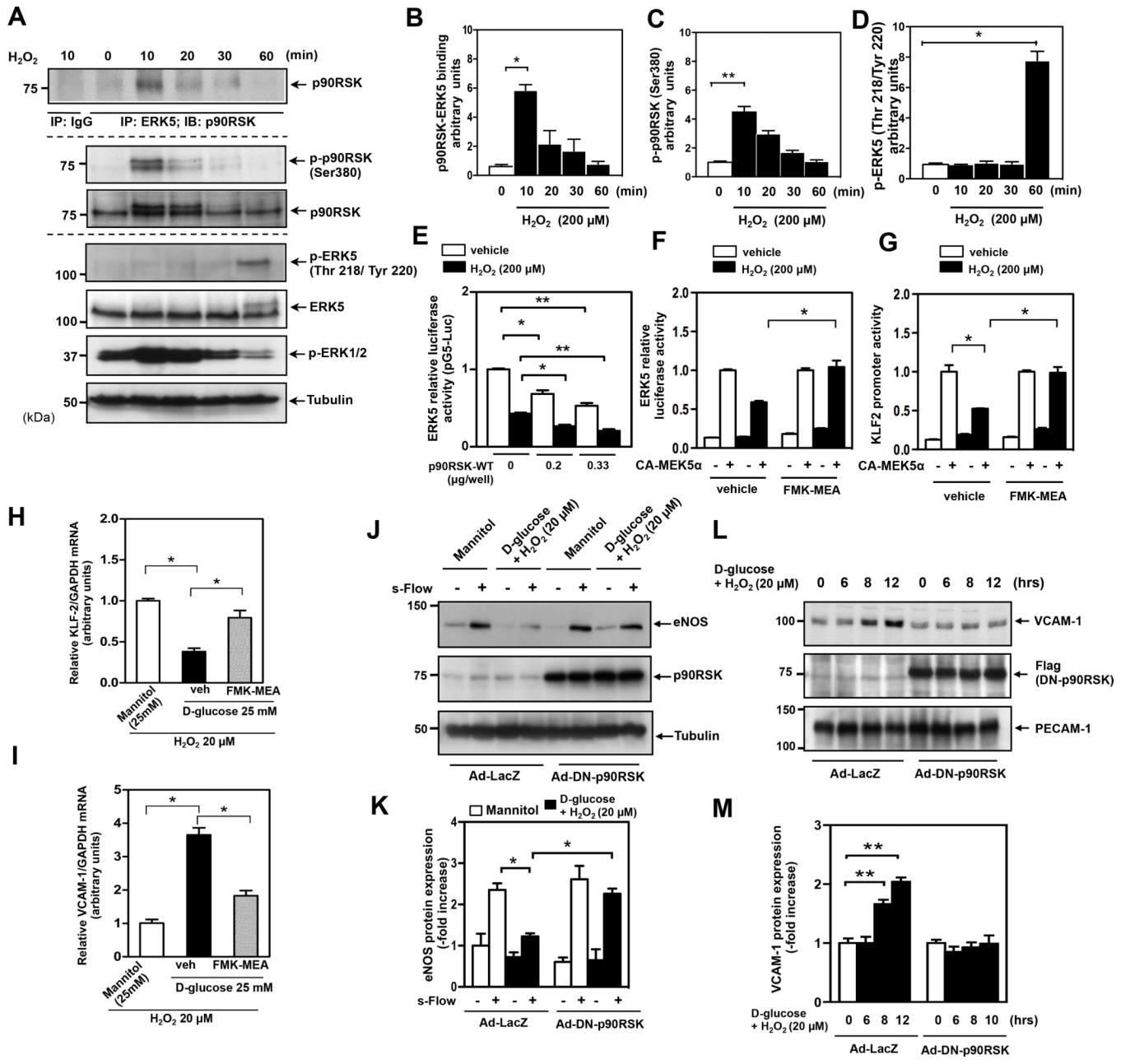

Figure 1.

p90RSK activation inhibits ERK5 transcriptional activation and regulates subsequent KLF2-eNOS expression and VCAM-1 expression. (A) HUVECs were treated with 200μM of H_2O_2 for indicated times. Cell lysate were immunoprecipitated with anti-ERK5 or IgG as a negative control. ERK5-bound p90RSK was detected by Western blotting using anti-p90RSK antibody (top). p-p90RSK, p90RSK, p-ERK5, ERK5, p-ERK1/2, and tubulin were detected using each specific antibody. (B, C, D) Densitometric quantification of: ERK5-bound-p90RSK (B), phosphorylation of p90RSK (C) and ERK5 (D). Results were normalized to the lowest association (B) phosphorylation level (C, D) within each set of experiments. Results are expressed relative to untreated cells (0 min), and relative to the corresponding band intensity of p90RSK (3rd from top) (C) or ERK5 (5th from top) (D) at each time point. Statistical significance was determined by comparing the average level of

the control group with that of each experimental data point. Experiments were carried out in triplicate using 3 different batches of HUVECs (B-D, mean ± SEM, n=3, **P*<0.05, ***P*<0.01 compared to control). (E) HUVECs were co-transfected with an empty vector or plasmids encoding p90RSK-WT, Gal4-ERK5, and the Gal4-responsive luciferase reporter pG5-Luc. Four hours later, Opti-MEM was replaced by supplemented M200 medium. Eight hours post transfection, cells were stimulated with 200μM H_2O_2 for 16hrs, and ERK5 transcriptional activity was assayed by the dual-luciferase reporter assay. p90RSK overexpression inhibited ERK5 transcriptional activity in a dose-dependent manner, and also enhanced H_2O_2-mediated reduction in ERK5 transcriptional activity. Luciferase activity was normalized relative to Renilla luciferase activity. The mean luciferase activity of an empty vector (vehicle treatment) was set as 1 (mean ± SEM, n=3). (F, G) HUVECs were co-transfected with plasmids encoding Gal4-ERK5 and the Gal4-responsive luciferase reporter pG5-Luc (F) or KLF2 promoter with luciferase (KLF2-Luc) and ERK5 wild type (G). Cells were also transfected with an empty vector or CA-MEK5α as indicated. Eight hours post transfection, cells were treated with FMK (10μM) for 3hrs, followed by stimulation with 200μM H_2O_2 for 16hrs. Finally, ERK5 transcriptional activity (F) and KLF2 promoter activity (G) were assayed by a dual-luciferase reporter assay (F-G, mean ± SEM, n=3). (H, I) MECs were pretreated with FMK-MEA (10μM, 3hrs), followed by stimulation with either HG/low H_2O_2 or Mannitol/low H_2O_2 as a control and (H) KLF2 mRNA and (I) VCAM-1 mRNA level were detected by qRT-PCR as described in methods (H-I, mean ± SEM, n=3). (J, K) HUVECs were transduced with either adenovirus vector containing DN-p90RSK or LacZ and 24hrs later, exposed to s-flow for 24 hrs in the presence or absence of a combination of high glucose (25mM) and low dose H_2O_2 (20μM). eNOS, p90RSK, and tubulin expressions were detected by Western blotting with specific antibodies (J). eNOS expression was quantified (mean ± SEM, n=3) (K). (L, M) MECs (passage 3) were transduced with either adenovirus vector containing DN-p90RSK or LacZ and 24hrs later, treated with a combination of high glucose (25mM) and a low dose of H_2O_2 (20μM) for indicated times. VCAM-1, PECAM-1 and p90RSK expressions were detected by Western blotting with specific antibodies (L). VCAM1 expression was quantified (mean ± SEM, n=3) (M).

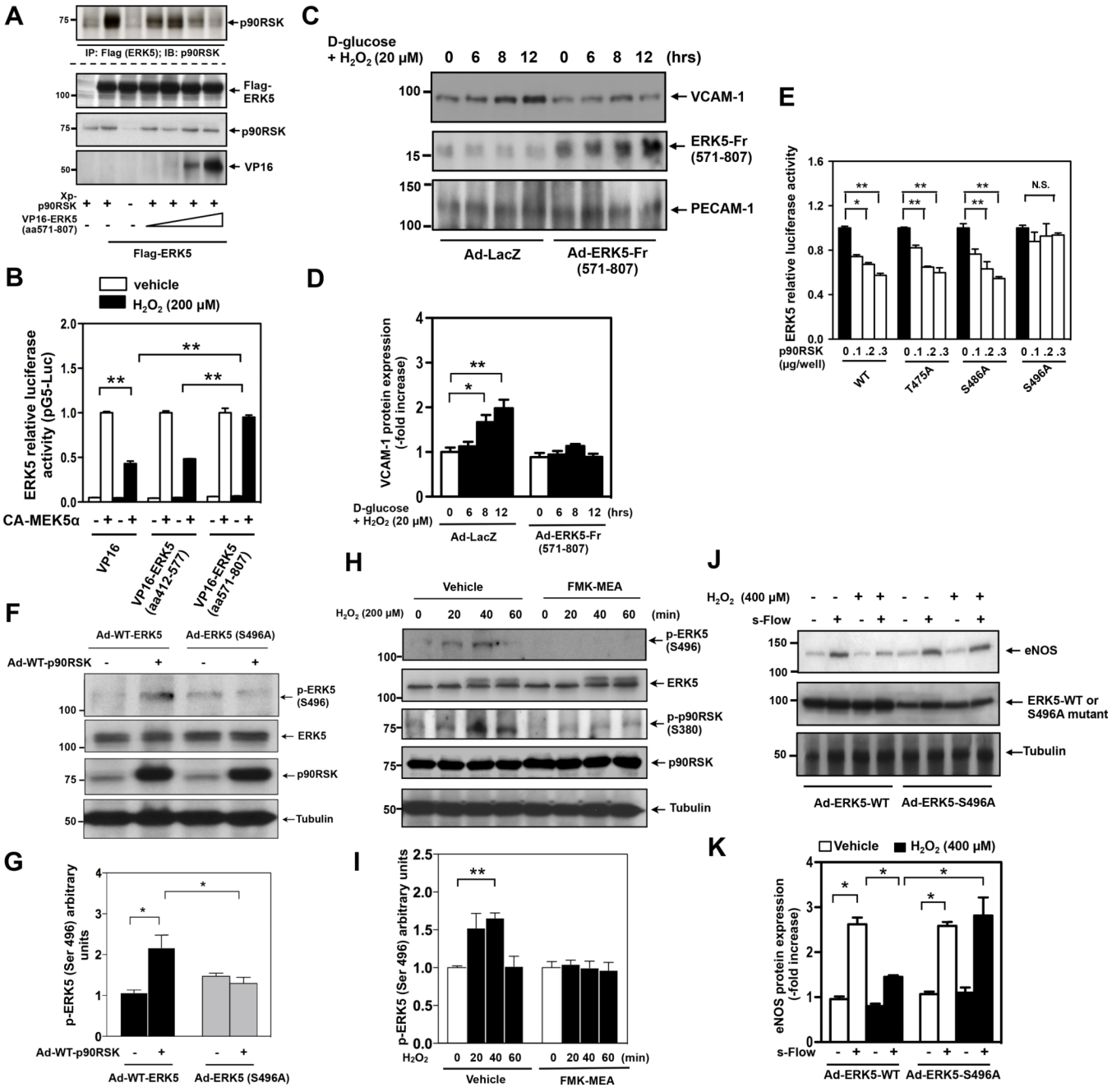

Figure 2.

p90RSK interacts with ERK5, phosphorylates ERK5-Ser496, and inhibits ERK5 transcriptional activity. (A) HeLa cells were co-transfected with Flag-tagged ERK5 wild type, Xpress-tagged wild type p90RSK, and a VP16-tagged ERK5 fragment (aa571-807) for 24hrs. Cell lysates were immunoprecipitated with anti-Flag, followed by immunoblotting with anti-p90RSK to determine p90RSK-ERK5 association (top). The expression of p90RSK, ERK5 and the ERK5 fragment were detected by immunoblotting with specific antibodies. The VP16-tagged ERK5 fragment inhibited p90RSK-ERK5 association. Data is a representative of 3 independent experiments. (B) HUVECs were co-transfected with an empty vector or plasmids encoding an ERK5 fragment (aa571-807) or (aa412-577), Gal4-

ERK5, and the Gal4-responsive luciferase reporter pG5-Luc. Cells were also transfected with an empty vector or CA-MEK5α as indicated. Twelve hours post transfection, cells were stimulated by 200μM H_2O_2 for 16hrs, and then ERK5 transcriptional activity was assayed by the dual-luciferase reporter assay as described above. Luciferase activity was normalized relative to Renilla luciferase activity, and the mean luciferase activity at the condition of CA-MEK5α transfection for vehicle treatment was set at the same level. Data are representative of three independent experiments (mean ± SEM, n=3). (C, D) MECs (passage 3) were transduced with either adenovirus vector containing ERK5 fragment aa571-806 (Ad-ERK5-Fr(571–807)) or Ad-LacZ. After 24hrs of transduction, cells were treated with a combination of high glucose (25mM) and a low dose of H_2O_2 (20μM) for indicated times. VCAM-1, PECAM-1 and ERK5 expressions were detected by Western blotting with specific antibodies (C). Densitometric quantification of VCAM-1 expression is shown (mean ± SEM, n=3). (D). (E) Transcriptional activity of the ERK5 S496A mutant cannot be inhibited by p90RSK. HUVECs were co-transfected for 24hrs with an empty vector or plasmids encoding p90RSK-WT with Gal4-ERK5-WT or a Gal4-ERK5-T475A, -S486A, or -S496A mutant, and a Gal4-responsive luciferase reporter. ERK5 transcriptional activity was assayed by a dual-luciferase reporter assay. Luciferase activity was normalized relative to Renilla luciferase activity, and the mean luciferase activity of an empty vector (p90RSK=0) was set as 1. Data are representative of three independent experiments (mean ± SEM, n=3). (F, G) HUVECs were transduced with either Ad-WT-ERK5 or Ad-ERK5 S496A mutant with Ad-p90RSK or Ad-LacZ as a control for 9hrs. ERK5-S496 phosphorylation, ERK5, p90RSK, and tubulin expression were detected by Western blotting with specific antibodies (F). Phosphorylation level of ERK5-S496 was densitometrically quantified (mean ± SEM, n=3) (G). (H, I) H_2O_2 increases ERK5-S496 phosphorylation via p90RSK activation. HUVECs were pre-treated with FMK-MEA (10μM) for 3hrs, then stimulated with H_2O_2 for indicated times. ERK5-S496 phosphorylation, ERK5, S380 p90RSK phosphorylation, p90RSK, and tubulin expression were detected by Western blotting with specific antibodies (H). Densitometric quantification was shown (mean ± SEM, n=3) (I). (J, K) HUVECs were transduced with either adenovirus vector containing ERK5 wild type (Ad-ERK5-WT) or ERK5-S496A mutant (Ad-ERK5-S496A). After 24hrs of transduction, cells were treated with or without H_2O_2 (400μM) and then exposed to s-flow for 24 hrs. eNOS, ERK5, and tubulin expressions were then detected by Western blotting with their specific antibodies (J). Densitometric quantification was shown (mean ± SEM, n=3) (K).

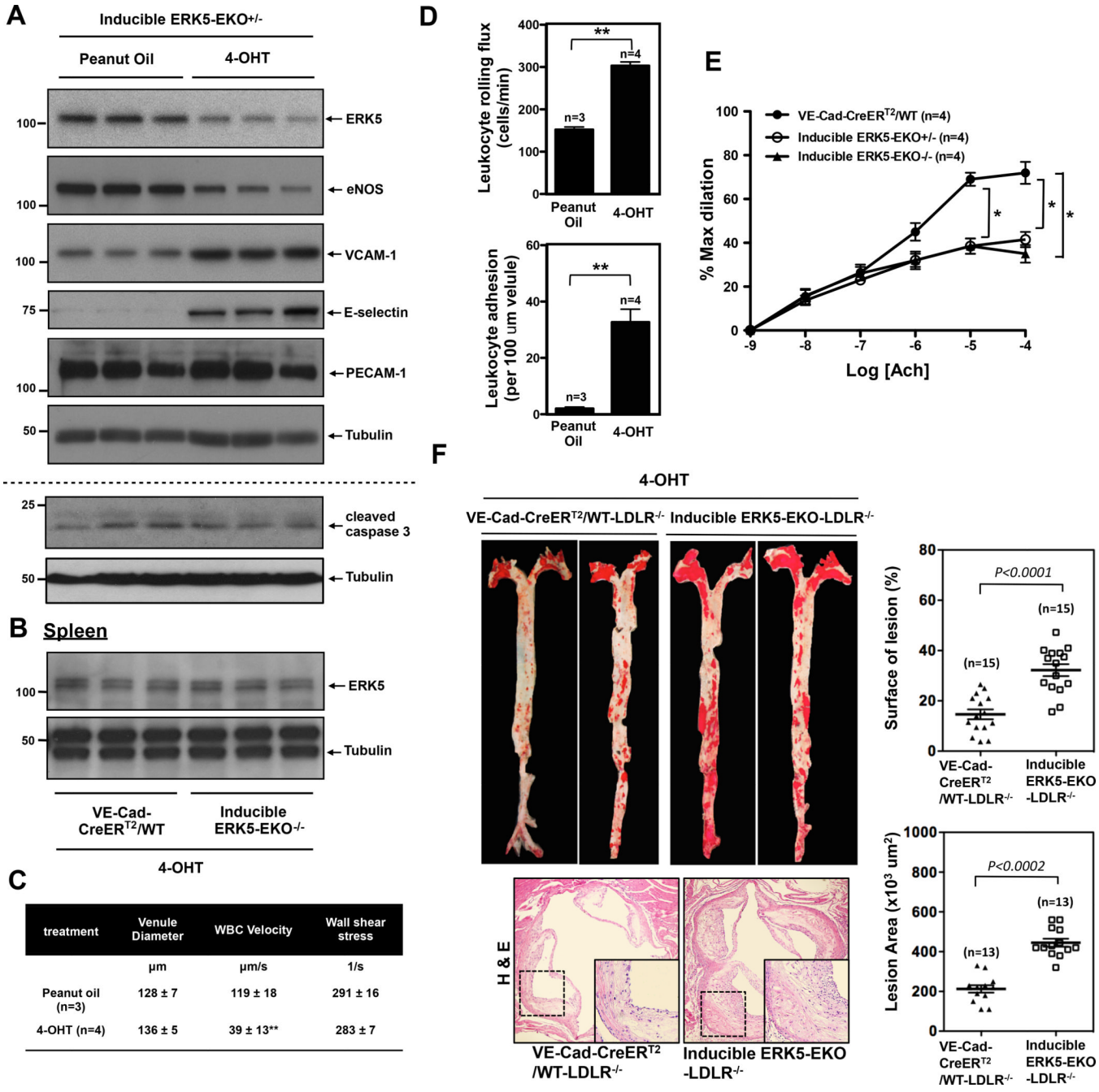

treatment	Venule Diameter	WBC Velocity	Wall shear stress
	μm	μm/s	1/s
Peanut oil (n=3)	128 ± 7	119 ± 18	291 ± 16
4-OHT (n=4)	136 ± 5	39 ± 13**	283 ± 7

Figure 3.

Reduced ERK5 expression in ECs in inducible ERK5-EKO mice increases leukocytes rolling, inhibits endothelium-dependent vasodilatation, and accelerates atherosclerosis formation in LDLR$^{-/-}$ mice. (A) The expression of ERK5, eNOS, VCAM-1, E-selectin, PECAM-1, and tubulin in cultured MECs isolated from two weeks of peanut oil or tamoxifen (4-OHT) treated inducible heterozygous ERK5-EKO$^{+/-}$ mice. MEC lysates were probed by Western blotting. (B) The expression of ERK5 and tubulin in the cell lysate obtained from the spleen of either VE-Cad-CreER^{T2}-WT or inducible ERK5-EKO$^{-/-}$ mice after two weeks of 4-OHT injections are shown. (C, D) Leukocyte rolling *in vivo*. Mice were anesthetized and injected with rhodamine 6G to label leukocytes. The mesentery was

externalized, and then Leukocyte rolling in venules 120 to 150μm in diameter was recorded with a digital video camera. Shown are quantified data of leukocyte rolling velocity (C), leukocyte rolling flux (D, top), and leukocyte adhesion (D, bottom). To analyze these parameters, image analysis software (NIS elements, Nikon) was used (n=3–4, mean ± SEM; **P<0.01 versus controls, non-parametric Wilcoxon T test). (Supplemental video 1 and Fig. 3D). (E) Endothelium-dependent relaxation to Ach. In tamoxifen treated VE-Cad-CreER^{TR}/wild type mice, endothelium-dependent vasodilatation to Ach was observed, but in the tamoxifen-treated inducible heterozygous ERK5-EKO$^{+/-}$ or homozygous ERK5$^{-/-}$ mice, vasodilatation was significantly reduced. The number of venules used per animals was 5 for each group. Data are shown as mean ± SEM, n=4 mice. (F) At the end of 16-week high-cholesterol diet, VE-Cad-CreER^{T2}/WT-LDLR$^{-/-}$ and inducible ERK5-EKO$^{-/-}$; LDLR$^{-/-}$ mice (Top, Left panel) showed increased oil red O–stained atherosclerotic lesions in the aorta and (Bottom, Left panel) increased H&E stained atherosclerotic lesions in the cross section of aortic valves. Each right panel graph presents mean ± SEM, (n=13–15, *P* value was calculated by non-parametric Wilcoxon T test).

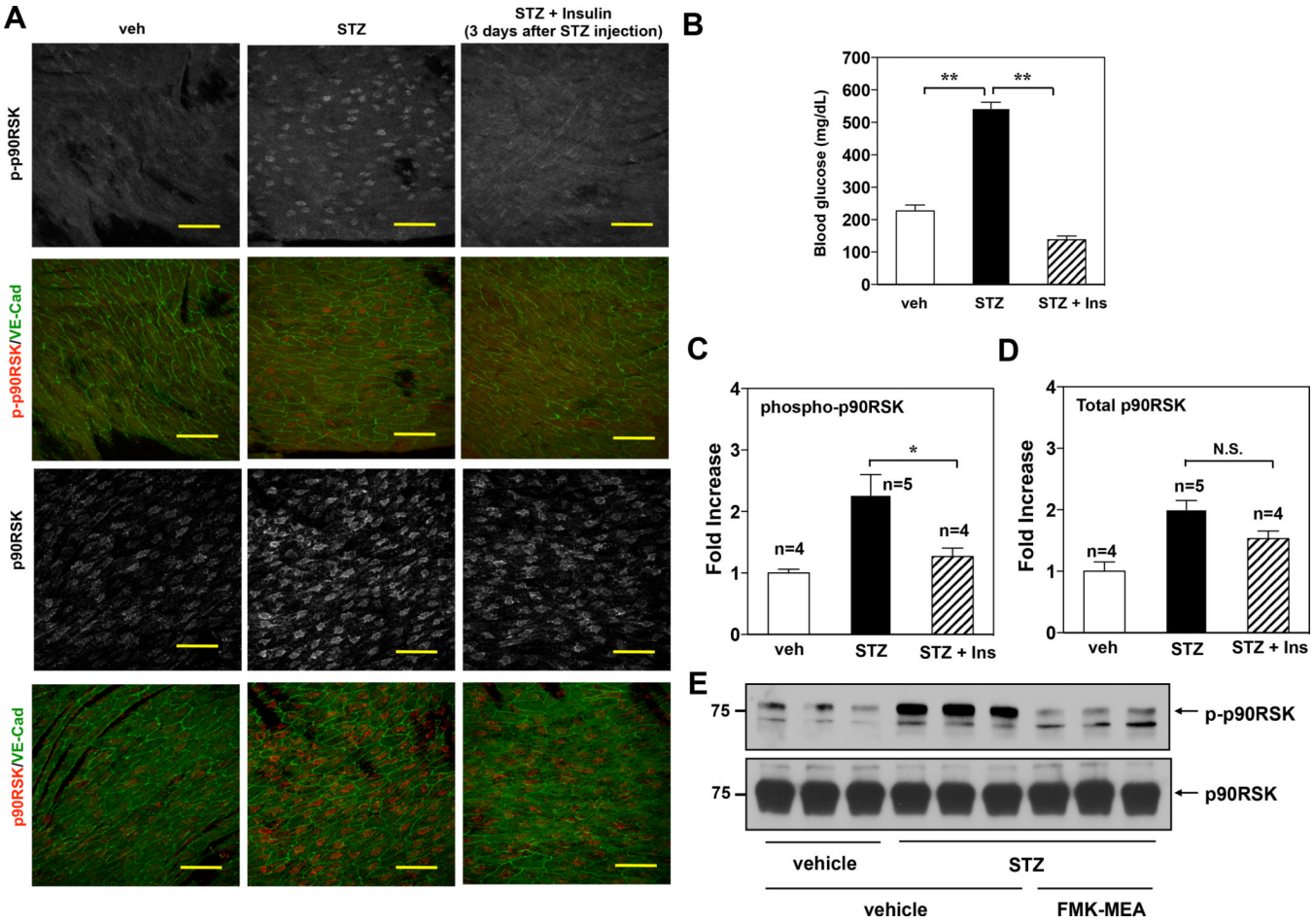

Figure 4.

p90RSK activation in mouse aortic arch and in MECs under hyperglycemia. (A) Confocal images of the endothelium of the greater curvature in mouse aortic arch of twelve-week-old C57BL/6 wild type. The *en face* specimen was double-stained with anti-VE-Cadherin (green) and anti-phospho-p90RSK (upper two panels, grey and red (merge)) or anti-total p90RSK (lower two panels, grey and red (merge)). Individual red signals as well as merged images are shown as indicated. Two weeks after STZ injection, blood glucose level was measured. Insulin (Ins) (Humalin N, twice daily, 5IU/kg) treatment was started after 3 days of STZ injection. Scale bars, 50μm. (B) Glucose tests in the blood of male mice after insulin treatment followed by injection of vehicle or STZ. (C, D) *En face* confocal images of diabetic and non-diabetic mice in s-flow area (greater curvature of aortic arch area) were obtained using the same image acquisition setting, and fluorescence intensity was quantified. Data are shown as means ± SEM. (E) C57BL/6 wild type mice were intra-peritoneally injected for three days with vehicle or STZ (100mg/kg/day), followed by vehicle or FMK-MEA injection as described in Fig.5A. After four days of FMK-MEA injection, MECs were isolated from the lungs of these mice as described in methods. Immediately, RIPA buffer was added to lyse the cells, then p-p90RSK (upper) and total p90RSK (lower) protein expressions were assayed by Western blotting using each specific antibody (n=3).

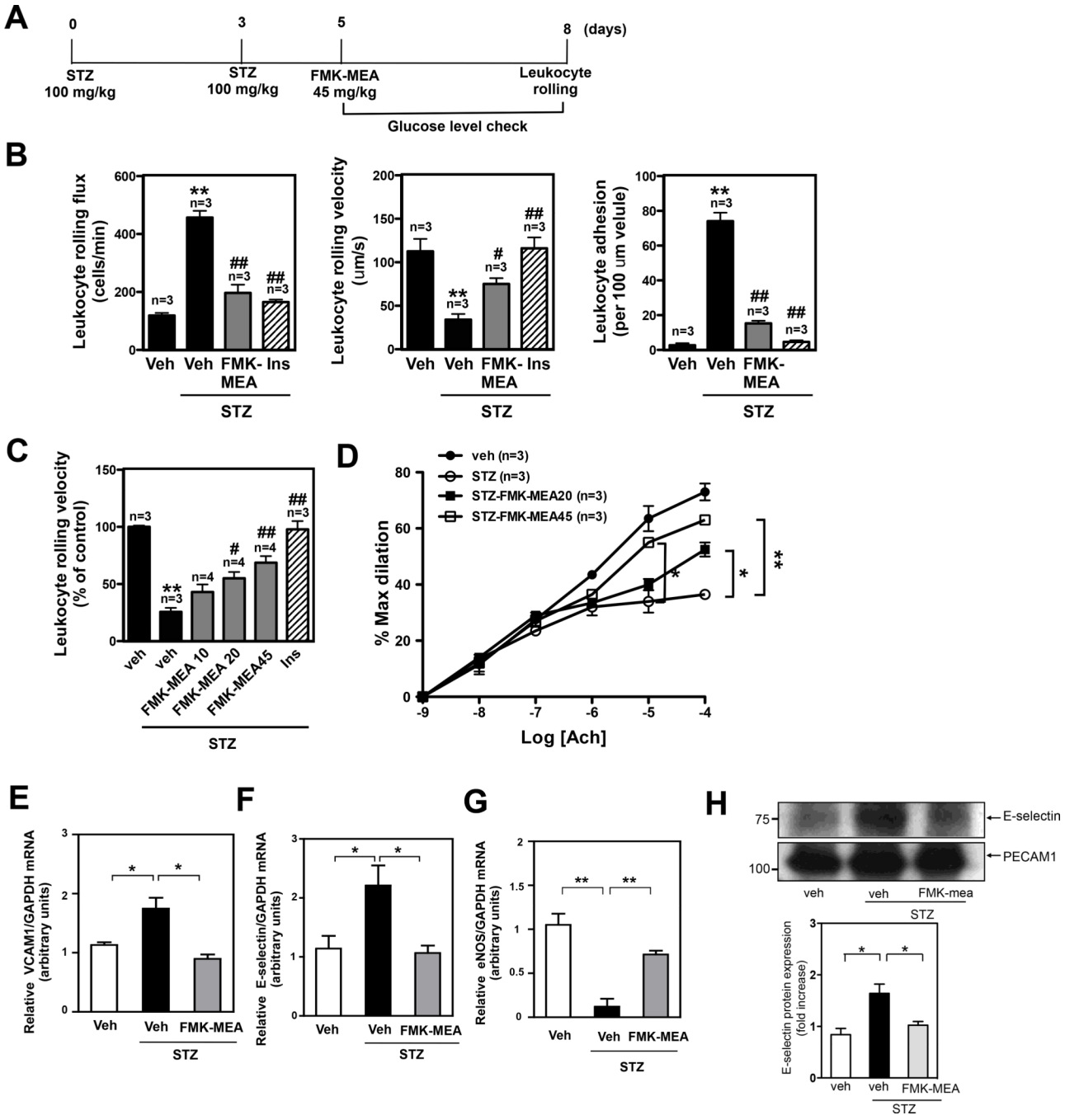

Figure 5.

The DM condition in STZ treated mice increases leukocyte rolling and reduces vasodilatation, and FMK-MEA treatment improves EC dysfunction with inhibition of EC inflammation and up-regulation of eNOS expression in these mice *in vivo*. (A) Scheme for STZ and FMK-MEA treatment. (B) Leukocyte rolling *in vivo*. Insulin (Humalin N, twice daily, 5IU/kg) treatment was stated after 4 days of first STZ injection. Mice were anesthetized and injected with rhodamine 6G to label leukocytes. Leukocyte rolling was imaged with a digital video camera for 2 min (n=3–4). Quantification of leukocyte rolling flux (number of rolling leukocytes passing a perpendicular line placed across the observed vessel in one minute), leukocyte rolling velocity, and leukocyte adhesion *in vivo*. To analyze

these parameters, image analysis software (NIS elements, Nikon) was used (mean ± SEM, n=4 mice; $^{**}P<0.01$ compared to vehicle with no STZ treatment group. $^{\#}P<0.05$, $^{\#\#}P<0.01$ compared with vehicle with STZ treatment group.). (Supplemental video 2) (C) Effects of FMK-MEA (10- 45 mg/kg/day, i.p.) and insulin on leukocyte rolling. Results are expressed relative to vehicle with no STZ treatment (100%). Shown is mean ± SEM (n = 3–4 mice); $^{**}P<0.01$ compared to vehicle with no STZ treatment group. $^{\#}P<0.05$, $^{\#\#}P<0.01$ compared to vehicle with STZ treatment group.) (D) Endothelium-dependent relaxations to Ach. Compared to -non-diabetic mice, vasodilatation in STZ-treated diabetic mice was significantly diminished. FMK treatment improved vessel reactivity to Ach in STZ-treated diabetic mice. Data are shown as means ± SEM, $^{**}P<0.01$ compared to STZ treatment group (n=3). (E-H) C57BL/6 wild type mice were intraperitoneally injected for three days with vehicle or STZ (100mg/kg/day), followed by vehicle or FMK-MEA injection as described in Fig. 5A. After four days of FMK-MEA injection, MECs were isolated from the lungs of these mice and then (for E-G) RNA was immediately extracted for real-time PCR (E) VCAM-1 mRNA (F) E-selectin mRNA (G) eNOS mRNA levels were detected by qRT-PCR as described in Methods. (H) RIPA buffer was added to lyse the cells, then E-selectin (upper) and PECAM-1 (lower) protein expressions were assayed by Western blotting using each specific antibody. Quantification of E-selectin protein was expressed as the relative ratio compared to PECAM-1 bands. Data (E-H) are shown as means ± SEM, n=3.

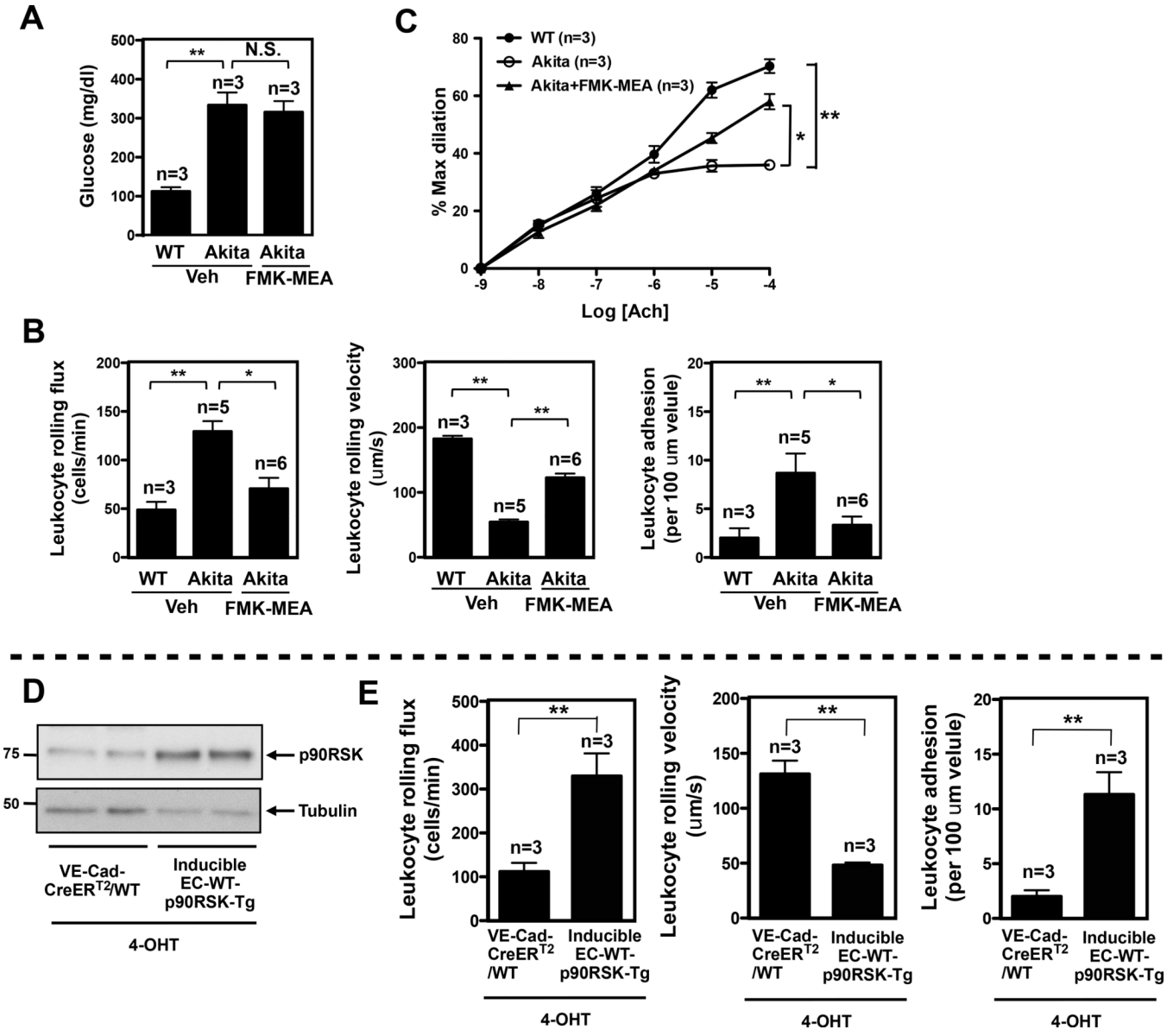

Figure 6.

DM condition in Akita mice and inducible endothelial specific wild type p90RSK transgenic mice increase leukocyte rolling and reduce vasodilatation. (A) Blood glucose levels in Akita male mice after vehicle and FMK-MEA treatment (45mg/kg/day, i.p.) for 4 days (mean ± SEM, n=3). (B) Quantification of leukocyte rolling flux, leukocyte rolling velocity, and leukocyte adhesion *in vivo*. To analyze these parameters, image analysis software (NIS elements, Nikon) was used (mean ± SEM, n=3–6). (Supplemental video 3) (C) Endothelium-dependent relaxations to Ach. FMK treatment improved vessel reactivity to Ach in Akita diabetic mice (means ± SEM, n=3 mice). (D) The expression of p90RSK and tubulin in cultured MECs isolated from two weeks of peanut oil- or 4-OHT-treated inducible EC-WT-p90RSK-Tg or VE-Cad-CreER^{T2}-WT mice. MEC lysates were probed by Western blotting. (E) Quantification of leukocyte rolling flux, leukocyte rolling velocity, and leukocyte adhesion in the 4-OHT treated inducible EC-WT-p90RSK-Tg or VE-Cad-CreER^{T2}-WT mice (mean ±SEM, n=3; $^{**}P<0.01$ based on non-parametric Wilcoxon T test). (Supplemental video 4)

A

	Genotype and treatment	Venule Diameter	WBC Velocity		Wall shear stress
		μm	μm/s		1/s
+ 4-OHT	VE-Cad-CreER^{T2}/WT + veh	125 ± 7	133 ± 17		288 ± 14
	Inducible ERK5-EKO-/- + veh	121 ± 5	39 ± 14**	N.S.	285 ± 4
	Inducible ERK5-EKO-/- + FMK-MEA	116 ± 4	47 ± 12**		287 ± 7
	Inducible ERK5-EKO-/- + veh	122 ± 6	36 ± 12**	N.S.	283 ± 5
	Inducible ERK5-EKO-/- + STZ + FMK-MEA	121 ± 8	39 ± 9**		285 ± 9

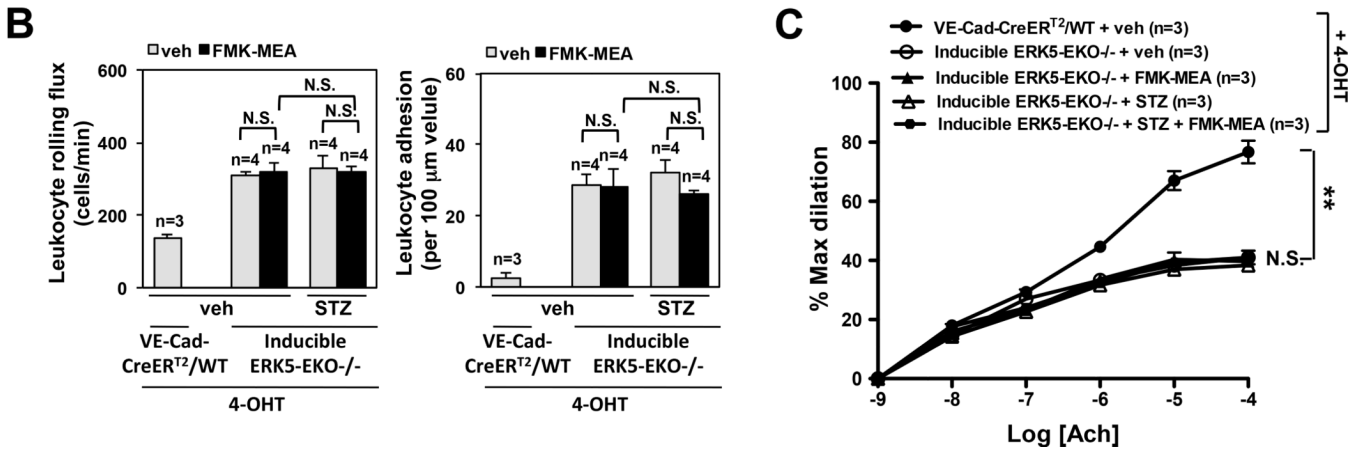

Figure 7.

FMK-MEA is ineffective in tamoxifen treated homozygous inducible ERK5-EKO$^{-/-}$ mice. (A) After 2 weeks of tamoxifen (4-OHT) treatment, inducible ERK5-EKO$^{-/-}$ mice were made hyperglycemia by intraperitoneal injection (100mg/kg) of streptozotocine (STZ) twice at days 0 and 3 (Fig.5A). At the third day of vehicle or STZ injection, both VE-Cad-CreER^{TR}/wild type and inducible ERK5-EKO$^{-/-}$ were injected with vehicle or FMK-MEA (45mg/kg/day) for three more days, and leukocyte rolling was examined. Quantification of leukocyte rolling velocity (A), rolling flux (B, left), and adhesion (B, right) *in vivo* is shown. To analyze these parameters, image analysis software (NIS elements, Nikon) was used (n = 3–4, mean ± SEM; ** P<0.01 versus controls). (Supplemental video 5) (C) Endothelium-dependent vasodilation by Ach. In the 4-OHT treated VE-Cad-CreER^{TR}/wild type mice, vasodilation by Ach was observed. However, in the 4-OHT-treated inducible homozygous ERK5-EKO$^{-/-}$ mice, vasodilation by Ach was significantly dampened. Both in the presence and in the absence of STZ injection, FMK-MEA failed to improve the vessel reactivity. For each group, 5 venules per animals were used for analysis (means ± SEM, n=3–5).

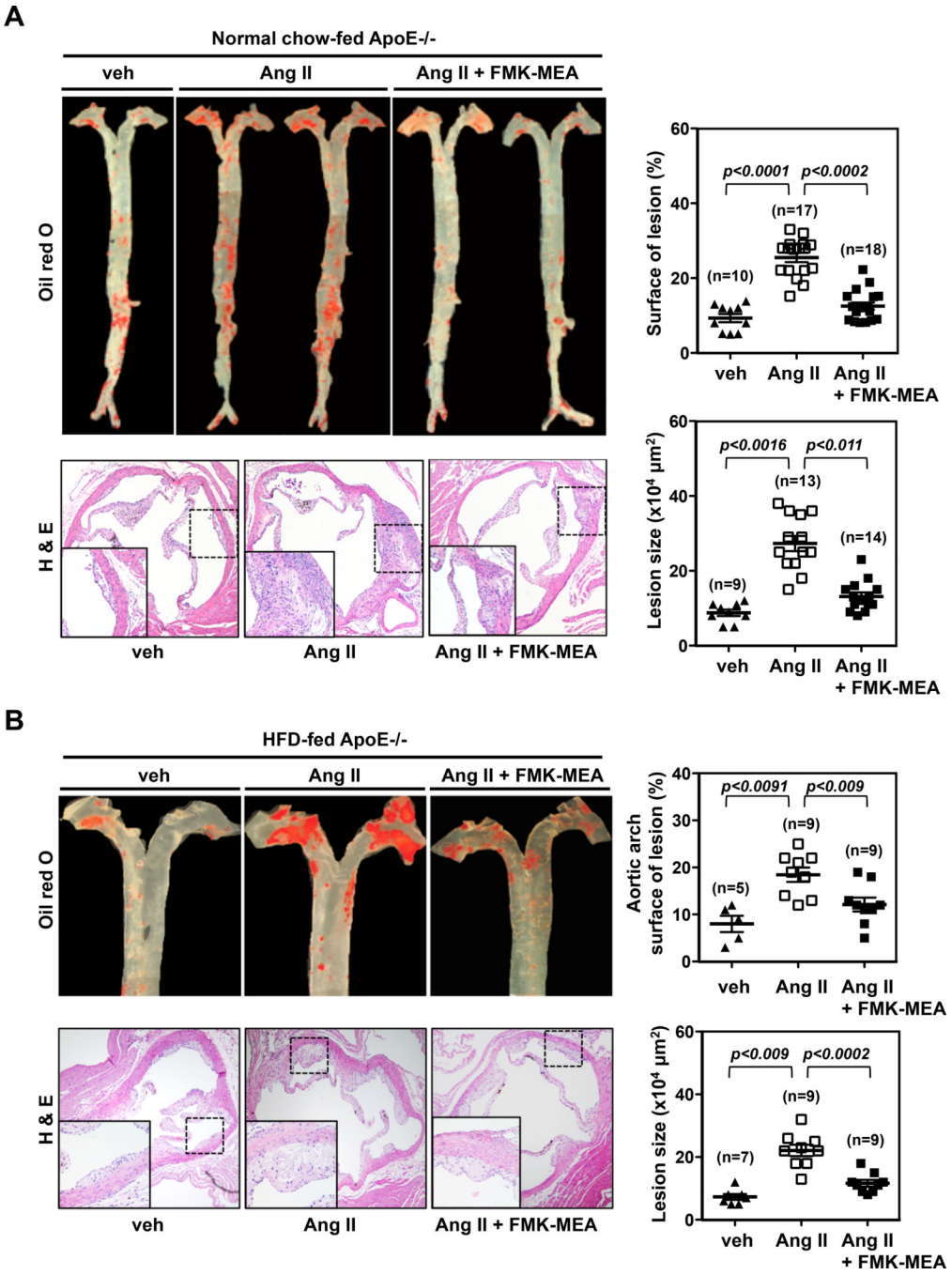

Figure 8.

FMK-MEA treatment inhibits atherosclerosis formation. (A, B) ApoE-KO mice receiving vehicle, AngII, or AngII + FMK-MEA under (A) normal chow diet or (B) high-fat diet for 28 days show (Top, Left panel) atherosclerotic lesions in the aorta with oil red O staining and (Bottom, Left panel) atherosclerotic lesions in the cross section of aortic valves with H&E staining. Each right panel graph presents mean ± SEM values (n=5–14).